

A GdBCO bulk staggered array undulator

M Calvi¹ , M D Ainslie² , A Dennis², J H Durrell² , S Hellmann¹,
C Kittel^{1,3} , D A Moseley² , T Schmidt¹, Y Shi²  and K Zhang¹

¹ Paul Scherrer Institute, Villigen PSI, Switzerland

² University of Cambridge, Trumpington Street, Cambridge, United Kingdom

³ University of Malta, Msida, Malta

E-mail: marco.calvi@psi.ch

Received 30 September 2019, revised 11 November 2019

Accepted for publication 25 November 2019

Published 11 December 2019



Abstract

The Insertion Device group of the Paul Scherrer Institute has started an R&D program on a high temperature superconducting undulator to reduce the period length and increase the undulator's magnetic field well beyond the present capability. Simulation results for a 10 mm period and 4 mm magnetic gap staggered array of GdBCO bulks predict peak magnetic field above 2 T. Building on the existing working principle of undulator design and simulated performance, the first experimental results of a 5 period 6.0 mm gap short undulator measured in the new test facility available at the University of Cambridge will be presented together with details of the experimental setup and sample preparation.

Keywords: FELs, synchrotron light source, insertion devices, HTS

(Some figures may appear in colour only in the online journal)

1. Introduction

Third generation light sources [1] maximised the number of straight sections to insert wigglers and undulators [2] between the arcs of the ring, thus increasing the number and the quality of the synchrotron radiation sources beyond dipole magnets. This is at the origin of the name *insertion devices* regularly used in the accelerator community to indicate both instruments. Today, undulators are the most used and efficient source of synchrotron radiation. There are three main parameters which characterise an undulator: its length (L), the period length (λ_u) and the deflection parameter (K) proportional to the peak magnetic field (B_0), which define the radiation wavelength through the following fundamental equation (valid for planar undulators)

$$\lambda = \frac{\lambda_u}{2n\gamma^2} \left(1 + \frac{1}{2}K^2 \right), \quad (1)$$


where γ is the Lorentz factor of the relativistic electron and n

is the harmonic number

$$K = \frac{B_0 e \lambda_u}{mc 2\pi} \quad (2)$$

e and m are respectively the charge and the mass of the electron.

Free electron lasers (FELs) are complementary sources of synchrotron radiation dedicated to experiments with femto second pulses where high coherence and high brightness are mandatory. Recently, the regime of the atto-seconds has been demonstrated [3, 4] which allows a new class of experiments. To perform the lasing process, a bright source of electrons is required together with a linear accelerator (linac) and a long undulator, see [5, 6]. While in a synchrotron an undulator source of >50 periods is sufficient to deliver photons to an experiment, in an FEL designed for lasing in the Ångström wavelength range (hard x-ray regime) the number of periods required is usually above 3000 [7–11]. Despite the attempt to lase at high harmonics [12], up to now all facilities have been designed to operate on the fundamental wavelength ($n = 1$) and realistically in future specifically designed beamlines it will be possible to reach the 3rd or maximum the 5th harmonic.

 Original content from this work may be used under the terms of the [Creative Commons Attribution 3.0 licence](https://creativecommons.org/licenses/by/3.0/). Any further distribution of this work must maintain attribution to the author(s) and the title of the work, journal citation and DOI.

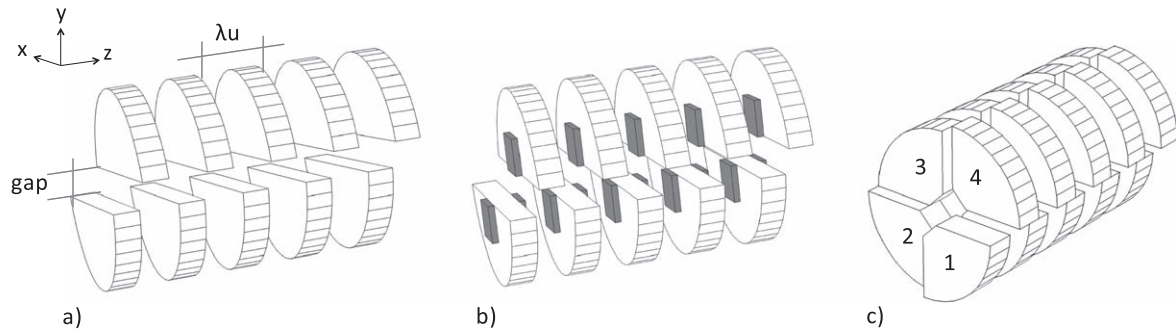


Figure 1. (a) The staggered array undulator geometry as proposed by Kinjo and co-workers and as it is also adopted for the test presented in this paper. (b) A new hybrid staggered array undulator, where ferromagnetic poles (dark-grey) positioned at the peak undulator field helps increasing its strength. (c) A new helical geometry which extends the staggered array to two dimensions. The round bulks are now cut in four pieces (1, 2, 3 and 4) and relatively shifted of $\lambda_u/4$ along the z-axis.

1.1. Undulator technology

In-vacuum permanent magnet undulators, operated either at room temperature (IVU) or at cryogenics temperature (CPMU) (77–135 K), are the state of the art technology reaching high photon energy and highly collimated photon beams. They are required in medium energy storage rings (<3 GeV) to achieve 40 keV photon energies [13]. This is possible using the high resonance harmonics of a CPMU. This requires a high degree of accuracy in the field profile, with a RMS phase error parameter [14] of $<2^\circ$.

In the last decade superconducting undulators based on NbTi have been developed both in Europe [15] and in the US [16]. For period lengths above 15 mm, they are more effective in generating large magnetic field than CPMU [17]. For lower period lengths alternative superconductors have to be used. Nb₃Sn has been magnetically tested in Berkeley lab [18] recently but its 19 mm period length chosen for the parameters of LCLS2 [19] does not allow a direct assessment of the very short period length regime focused on in this paper. Superconducting undulators have the advantage of being less sensitive to radiation than permanent magnets, which may experience irreversible field losses due to interaction with high energy particles and their associated hadronic shower.

Due to the large investment involved in the construction of an FEL, an European project, XLS [20], has been started with the aim of designing a compact FEL in the hard x-ray regime to increase the availability of those instruments by reducing the size of the infrastructures and consequently the costs of the whole installation. The R&D activities on short period superconducting undulators at PSI started for application in FELs, where the operation on low harmonics relaxes the requirements on the phase error ($<10^\circ$) and the low re-rate of classical copper linac (100–120 Hz) does not impose high heat load to the devices. Meanwhile, the synchrotron community has also expressed significant interest for this development and the challenging implementation of this superconducting undulator in a storage ring will be evaluated too. Within the XLS collaboration, PSI decided to investigate the staggered array configuration [21] following the design by

Kinjo and co-workers [22, 23], where for the first time it was proposed to implement HTS bulks in place of iron poles and/or permanent magnets [24], see figure 1(a)

2. The superconducting staggered array principle

The working principle of a superconducting staggered array undulator (SSAU) is to shape the uniform field of a solenoid into an undulator field (B_0). One of the advantages of a SSAU to its normal conducting option [21] is the possibility to operate without a solenoidal background field. The most effective procedure to obtain this result is to field cool (FC) the HTS bulks in a superconducting solenoid. The current on the solenoid is slowly driven to zero and the variation of the field is compensated by an induced current on the HTS effectively trapping a magnetic field. In a SSAU, due to the specific geometry of the HTS bulks arrangement—*staggered geometry*—even though the upper and the lower rows of the HTS bulks are identically magnetised, the magnetic fields do not cancel each other but add together to produce B_0 thanks to their relative positional shift of $\lambda_u/2$. In a standard permanent magnet arrangement it is possible to introduce magnets with inverse magnetisation and further increase the undulator field (with the eventual addition of iron poles as well). Unfortunately, this has not been considered as a realistic option for a SSAU as the HTS bulks require an *in situ* magnetisation. Furthermore, a complex mechanical installation operated in cryogenic temperatures is required to allow manipulation of those blocks, as proposed in [25, 26] where alternative geometries are presented.

A λ_u of 10 mm and a magnetic gap of 4 mm (distance between the flat edge of the upper and the lower row) have been selected as ambitious parameters because both CPMU and existing NbTi undulators do not deliver enough field (<1 T) for the design of a compact FEL. COMSOL and ANSYS have been used to solve the magnetisation problem: the first implements the popular H-formulation while the second uses a new approach based on the A–V formulation [27]. In this paper, the main results of the design optimisation are introduced, more details can be found in [28]. In figure 2

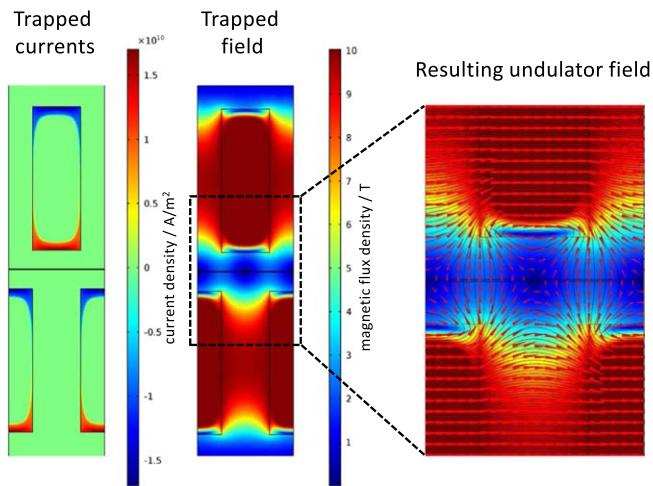


Figure 2. The details of an undulator period (10 mm): on the left the trapped currents, in the middle the trapped field and on the right the magnetic vector plot where the negative and positive poles of the undulator are visible. This is the result of a 3D simulation model where periodical boundary conditions are applied.

the results of a 3D model with periodic boundary conditions are presented where the current and trapped field are highlighted. Zooming into the actual gap where the relativistic electrons will be confined, it is possible to clearly identify the undulator field produced by the flat upper and lower edge of the HTS bulks. As in the original Kinjo's design, the half moon geometry has been selected because the round shape is the natural way in which those crystals are grown. Furthermore, the solenoid aperture is also round and should be as small as possible to minimise the stored energy and the stray fields. Nevertheless this might not be the optimum geometry to introduce the required pre-stress [29] to compensate the large tensile stresses induced by the Lorentz forces. For this test the diameter of 30 mm and the thickness of 4 mm has been selected. For both parameters the optimum depends on assumed $J_c(B)$ values. However, there is only a weak dependence in behaviour for the diameter while the thickness plays a more substantial role [28]: indeed for high performance bulks measured by the company ATZ the optimum thickness is lower than $\lambda_u/2$, whereas for lower J_c it gets closer to $\lambda_u/2$.

Better understanding of the working principle acquired during the optimisation work has triggered ideas for new designs. First, the reduced thickness gives room for additional ferromagnetic poles of 1 mm, see figure 1(b), which is a simple and effective way to further increase the undulator field. Furthermore, the small volume of magnetic material required allows for solutions implementing gadolinium, dysprosium or holmium which are usually not affordable in large superconducting accelerator magnets. Second, an alternative design based on the helical geometry was discovered, see figure 1(c). This solution is also an extension of the staggered array: the original geometry has one pair of rows facing each other, this one has two pairs of rows. This is only a preliminary idea and a detailed optimisation study is required to understand its full potential.

3. The undulator sample and its instrumentation

The 10 period undulator presented in figure 3(a) was designed to fit the requirements of the 12 T cryogen free magnet available at the University of Cambridge. Although, it is not longer than its homogeneous field region ($<2\%$) it has enough periods to judge the undulator field quality. Nevertheless, the results presented in this paper were obtained on a shorter sample with a gap of 6 mm (see figure 3(b)) to simplify and speed up the commissioning of the instrumentation. The bulks were not glued on the sample holder because they will be later reused for the assembly of the first standard short sample. This allows relative motion of the different sample components and leaves open the possibilities of local source of heat generated by friction which can give rise to a thermal run away (quench). The absence of pre-stress limits the highest field which can be applied to the sample before exceeding the tensile strength and damaging the sample [29]. For this reason, the field was never raised above 7 T during the entire test campaign. A detailed simulation of the stress state of the sample during the magnetisation process pointed out two different magnetisation procedures which we refer as mono-polar and bipolar magnetisation. In the majority of the applications, the external field used to magnetise the bulks is finally switched off and the superconducting device, usually referred to as a superconducting permanent magnet, works in persistent mode. This example is a case of mono-polar magnetisation: more specifically we refer to mono-polar magnetisation when the undulator is cooled down in a field of magnitude B and which is later lowered to zero and we refer to bipolar magnetisation when the FC is done at $B/2$ and the field is lowered to $-B/2$. For the same field change ΔB , the undulator field obtained is very similar (slightly higher for the mono-polar) but the stress state is completely different: in the mono-case the bulk ends in a fully tensile stress while in the bi-mode it ends in compression state. This has important consequences as the bulks are more vulnerable in tensile than in compressive stress and it allows bipolar magnetisation with ΔB of 10 T in unreinforced samples which would crack in mono polar mode.

In figure 4 the sample holder is presented: it consists of copper disks 5 mm thick where the slot for the bulk crystal is machined out. Six holes are drilled on the outer radius to hold them together and a central hole of 5 mm diameter gives the space for measuring the undulator field. Ten disks are assembled for this test and 21 will be assembled for the future tests. The Hall probe sketched in figure 5 is used to measure the three components of the magnetic field on the undulator axis. It is called a $x3yz$ -probe because it is designed to measure the solenoidal component (z), the undulator field (y) in three different y positions (one on axis and two off axis of $100 \mu\text{m}$) and the residual field error components (x). The probe is supported by a carbon-fibre tube which can be rotated manually around the z -axis to minimise the angle error and displaced along this z -axis with a stepper motor. A linear Heidenhain encoder will be shortly added to reach the micrometer positioning accuracy required for the qualification of an undulator. The five Hall elements

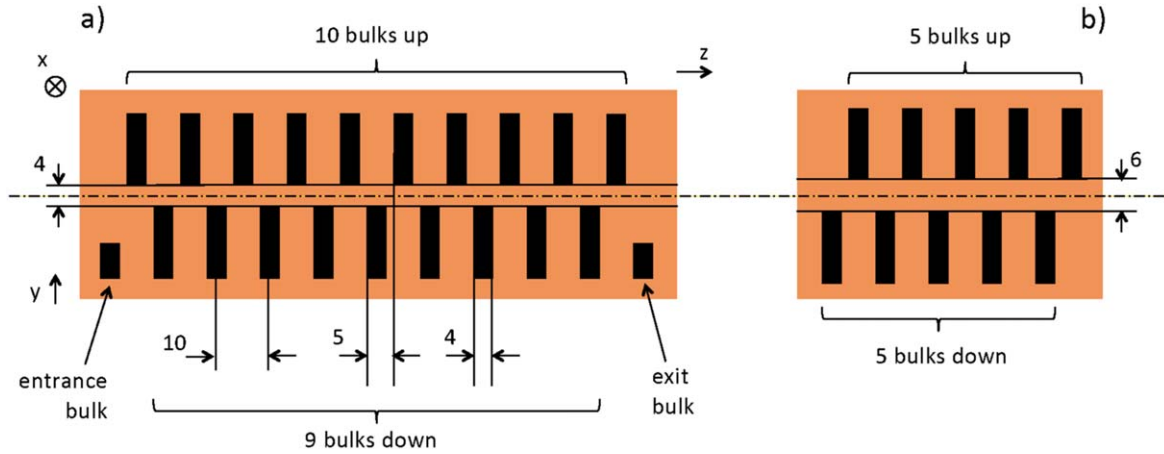


Figure 3. (a) On the left the standard undulator geometry, optimised to fit in the 12 T solenoid available at the university of Cambridge. Several samples of this size will be tested for direct comparison of their magnetic performance. (b) On the right the first sample tested where a larger aperture of 6 mm is used to simplify the commissioning of the new designed instrumentation. Its crystals size is compatible with the regular holder and those crystals will be reused for the test of the first standard sample. In the picture the units are in mm.

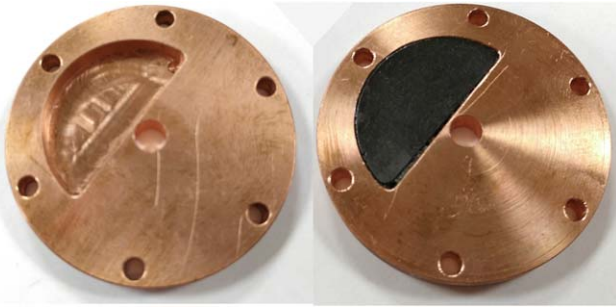


Figure 4. On the left the copper disk alone and on the right the GdBCO crystal machined to its final shape and inserted into the groove of the copper disk. There are six holes on the outer radius for bolting the disks together and a central one for leaving the space required for measuring the field.

are powered in series with $100 \mu\text{A}$ and read one by one with a multiplexer connected to a Keithley Nano-voltmeter. To minimise offsets and thermal voltages the current is reversed and each measurement point is always the average (with opposite signs) of the two readings. The sample is installed in a VTI and it is direct cooled with a stream of cold helium from the bottom. A heater and two thermometers, one at the bottom and one at the top, are mounted onto the undulator. This allows the temperature to be accurately stabilised to the given target value via a feedback loop minimising thermal gradients.

4. The test results

After field cooling the sample in 7 T down to 10 K, the solenoid is ramped down in steps of 1 T and the field profile is measured. In figure 6(a) an example of raw data is presented where the signal of the three y-probes overlaps nicely after shifting them in the z axis according to their spacing.

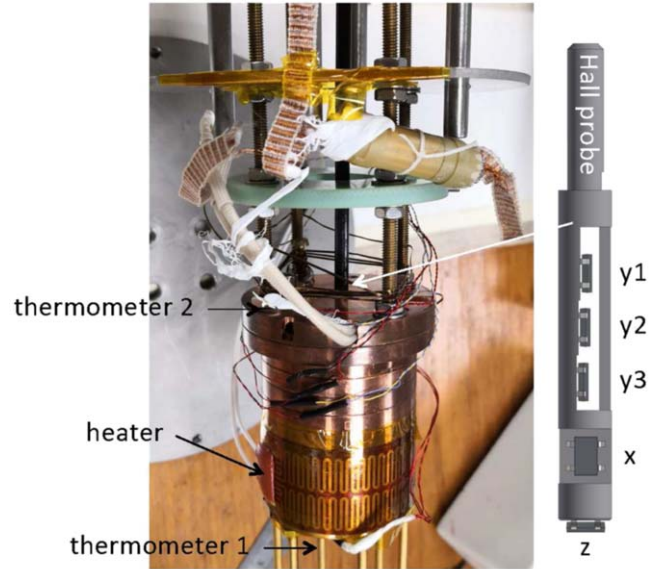


Figure 5. The undulator sample ready to go into the 12 T solenoid for the cold test. The main instrumentation is highlighted: on the right a sketch of the probe with the five Hall elements, at the bottom and at the top the thermometers used for stabilising the sample temperature together with the heater.

The profile is qualitatively as expected from the simulations: the maximum field is located at both ends. The limited number of periods requires a dedicated data analysis: the five most central local maxima are identified with the first five letters of the alphabet and the four peak values defined as $1/2(B_a - B_b)$ are reported as a function of the solenoidal field variation ΔB , see figure 6(b). The simulation results are reported on the same plot for an easy assessment of the predictive accuracy. The spread of the four values indicates a large variation among the contribution of the different bulks. This is due to the variation of the J_c properties and the geometrical tolerances of this first sample.

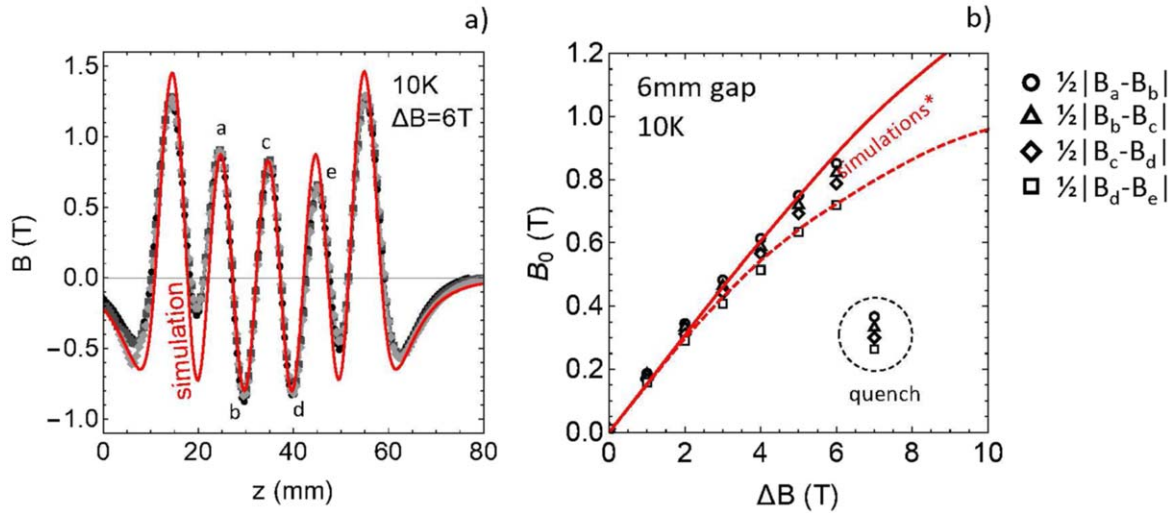


Figure 6. (a) On the vertical axis the magnetic field (B) recorded with the Hall elements y_1 , y_2 , y_3 (markers) and the simulated values (solid redline) as a function of the vertical position (z). The good overlap of the three signals indicates that the position of the probe in the y -axis was accurate within one tenth of a mm. The discrepancy among the signals in the first 10 mm (z) is an artefact of the positioning system. A linear encoder will be implemented shortly to prevent those kind of issues. (b) The summary of the first test run, performed with FC at 7 T after reaching the temperature of 10 K. The undulator magnetic field value (B_0) is presented as a function of the solenoidal field change (ΔB) as indicated in the legend. The solid redline is the simulation result using the scaling laws (J_c versus B) provided by the company ATZ at 4.2 K while the dashed redline is from the scaling laws measured in Cambridge at 40 K and scaled to 10 K with a factor $\times 2.5$.

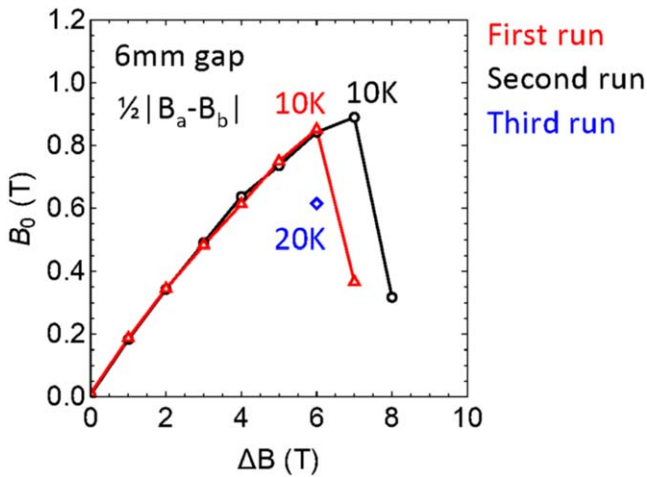


Figure 7. The summary of the three test runs: the first two at 10 K, the third at 20 K. The increased field from the 1st to the 2nd indicates a possible training quench mechanism which could be explained by bulk motion due to the lack of impregnation. The third run at 20 K highlights that the reduced J_c is not compatible with the high performance expected by this undulator.

In particular, the position of the straight edge of the bulks with respect to the undulator centre was not accurately determined. However, it is too early to draw any definitive conclusions.

In the first run the undulator field was increasing regularly as the solenoidal field was reduced. At $\Delta B = 7$ T, the field profile measured showed a sudden reduction in the trapped field. A second run with field cooling at the reduced field value of 6 T and the same temperature of 10 K, was performed which clearly showed that the sample was not permanently damaged. A third run was finally done at 6 T at

the increased temperature of 20 K, this time no intermediate field profiles were recorded during the solenoid ramp down process. The summary of the three campaigns is reported in figure 7. The higher undulator field measured during the second campaign (~ 0.85 T) at the increased ΔB of 7 T indicates an underlying training mechanism which could be interpreted as bulk motion. Under the influence of the Lorentz forces the superconducting bulks can move if space is available and the retaining forces are too weak. A sudden motion induces a local heat dissipation and an increase of temperature which translates directly in a J_c reduction and a quench. A detailed analysis of the field loss indicates a very uniform reduction of the field which proves very good thermal coupling among the different bulks of the sample. A reduced training behaviour is expected after fixing the bulks permanently to the copper disks with epoxy. The third and last run was performed after field cooling at 6 T down to 20 K. The reduced J_c limits the performance as expected and indicates that 10 K is probably the upper limit for this application.

5. Conclusions and outlook

This initial test campaign shows that ReBCO bulks could transform undulator technology. It confirms the results of [23] ($B_0 = 0.85$ T, gap = 4 mm, $\Delta B = 4$ T, 6 K) and demonstrates that with higher solenoidal magnetisation field it is possible to generate much stronger undulator fields ($B_0 = 0.85$ T, gap = 6 mm, $\Delta B = 7$ T, 10 K). Figure 8 shows the comparison for 6 mm magnetic gap among permanent magnets and low temperature superconductors using the scaling laws published in the literature [30, 31]. The highest value obtained during this

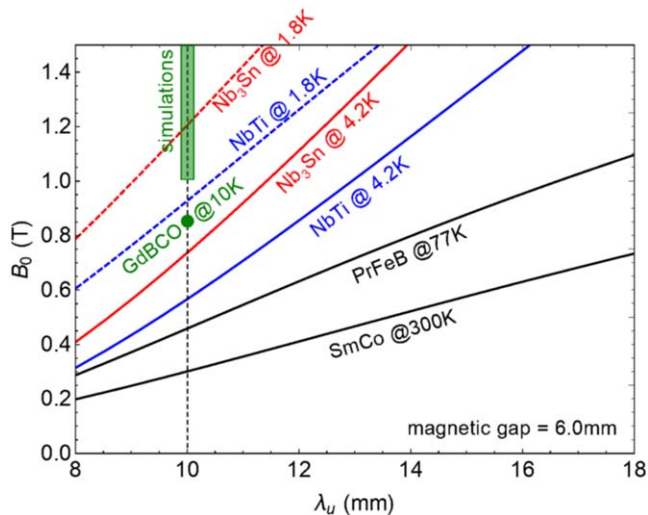


Figure 8. The scaling laws published in the literature are presented in the undulator field (B_0) versus the undulator period (λ_u) plane at 6 mm magnetic gap, for permanent magnets (SmCo), cryogenic permanent magnets (PrFeB) and low temperature superconductors (NbTi and Nb₃Sn). The highest value obtained during this campaign is plotted as well (green dot) together with the expected performance obtained in simulation between 4.2 and 10 K for different scaling laws published in the literature.

first test campaign (green dot) is presented together with the simulation results (green rectangle) which highlights the great potential but also the large uncertainty of the material parameters available. Higher performances are expected with reinforced bulk support to avoid training quenches. A standard 10 period short sample will be assembled shortly and tested at the nominal gap of 4 mm to confirm these preliminary results. This test will be the first of a series, planned to assess fundamental questions on the application of this technology in accelerator based light source. The first investigation will be a study of the magnetisation process in greater detail as a high degree of reproducibility (in the order of 0.1%) is required to operate the device as a light source. All origins of uncertainty should be identified and improved: the temperature, the temperature gradients and the current cycle during the magnetisation process and eventually other parameters not yet identified. The introduction of a temperature margin (flux freezing technique) and demonstration of its efficiency to prevent both field decay and local field variation due to small external heat load will be an important milestone for the project. The quality of the field profile from different industrial manufactures and different technologies (bulks versus tapes) will be investigated with a series of different samples. The maximisation of the field (K) achievable will be evaluated with the addition of ferromagnetic poles (CoFe, Gd, Dy, Ho) and the trade off between performances and complexity will be evaluated. The helical geometry will be tested for the first time as well, because of its relevance for compact FELs. The shrink fitting technique to introduce pre-stress in bulks will be investigated to reduce the tensile stress and to increase the undulator field in mono-polar magnetisation as well. Different sorting procedures will be studied to manufacture stack-tape-

bulks for minimising the spread of their performances and achieve higher field quality. After obtaining peak to peak field variations in the order of few percent (the quality of today permanent magnets), the efficiency of different optimisation algorithms shall then be evaluated: swapping, local period variation, pole height tuning, etc. Those manipulations will be expensive because of the low operating temperature and the time required to warm up and cool down the sample: the choice of optimum algorithms will be crucial to minimise the required number of steps but also ascertaining the correlation (cold to very cold correlation) between performance at 77 K versus 10 K operation might reduce the overall cost of the devices.

In conclusion, the Insertion Device group of PSI and the Bulk Superconductivity group of the University of Cambridge are looking forward to starting this new phase of the project with the aim of delivering the final design of a full scale undulator in 2021.

Acknowledgments

The authors would like to acknowledge T Tanaka and R Kinjo to share their experience on HTS undulators and S Reiche to highlight the great potential of a new SwissFEL beamline based on short period (10 mm) high K (>2) undulators. H Braun, O Bunk, L Patthey, L Rivkin, M Seidel, M Stambanoni and P Willmott for their constant support of the project. The University of Cambridge would like to acknowledge Henry Royce Institute Equipment Grant: EP/P024947/1. CompactLight has received funding from the European Union's Horizon 2020 research and innovation programme under grant agreement No. 777431.

ORCID iDs

M Calvi <https://orcid.org/0000-0002-2502-942X>
 M D Ainslie <https://orcid.org/0000-0003-0466-3680>
 J H Durrell <https://orcid.org/0000-0003-0712-3102>
 C Kittel <https://orcid.org/0000-0001-5527-1009>
 D A Moseley <https://orcid.org/0000-0001-7673-0024>
 Y Shi <https://orcid.org/0000-0003-4240-5543>

References

- [1] Namkung W 2010 *Proc. IPAC'10 (Kyoto, Japan)*
- [2] Clarke J A 2004 *The Science and Technology of Undulators and Wigglers (Oxford Series on Synchrotron Radiation)* (Oxford : Oxford University Press)
- [3] Huang S et al 1992 *Phys. Rev. Lett.* **119** 154801
- [4] Marinelli A et al 2017 *Appl. Phys. Lett.* **111** 151101
- [5] Schmäser P, Dohlus M, Rossbach J and Behrens C 2014 *Ultraviolet and Soft X-Ray Free-Electron Lasers* (Berlin: Springer) 978-3-319-04081-3
- [6] Willmott P 2019 *An Introduction to Synchrotron Radiation* 2nd edn (New York: Wiley) 978-1-119-28039-2
- [7] Milne C J et al 2017 *Appl. Sci.* **7** 720
- [8] Ishikawa T et al 2012 *Nat. Photon.* **6** 540–4

- [9] Weisand E and Decking W 2017 *Proc. FEL 2017 Santa Fe (USA)* pp 9–13
- [10] Kang H S *et al* 2017 *Nat. Photon.* **11** 708–13
- [11] Emma P *et al* 2009 First lasing of the LCLS x-ray FEL At 1.5 Å *Proc. PAC09 (Vancouver)*
- [12] Schneidmiller E A and Yurkov M V 2012 *Phys. Rev. Spec. Top. Accel. Beams* **15** 080702
- [13] Calvi M *et al* 2013 *J. Phys.: Conf. Ser.* **425** 032017
- [14] Walker R P 1993 *Nucl. Instrum. Methods* **335** 328–37
- [15] Casalbuoni S 2018 *Supercond. Sci. Technol.* **32** 023001
- [16] Ivanyushenkov Y *et al* 2017 *Phys. Rev. Accel. Beams* **20** 100701
- [17] Bahrtdt J and Gluskin E 2018 *Nucl. Instr. Methods Phys. Research, A* **907** 149–68
- [18] Arbelaez D 2017 private communication.
- [19] Emma P *et al* 2014 A plan for the development of superconducting undulator prototypes for LCLS-II and future FELs *FEL2014* (Switzerland: Basel) pp 649–53
- [20] XLS-Report-2019-004 27 June 2019 (https://compactlight.eu/uploads/Main/D5.1_XLS_Final.pdf)
- [21] Huang Y C *et al* 1992 *Nucl. Instrum. Methods A* **318** 765–71
- [22] Kii T *et al* 2012 *IEEE Trans. Appl. Supercond.* **22** 4100904
- [23] Kinjo R *et al* 2013 *Appl. Phys. Express* **6** 042701
- [24] Sasaki S 2005 The possibility for a short-period hybrid staggered undulator *Proc. 2005 Particle Accelerator Conf. (Knoxville, Tennessee)*
- [25] Tanaka T, Hara T and Kitamura H 2004 *Phys. Rev. Spec. Top. Accel. Beams* **7** 090704
- [26] Tanaka T, Tsuru R and Kitamura H 2005 *J. Synchrotron Radiat.* **12** 442–7
- [27] Zhang K, Hellmann S, Calvi M, Schmidt T and Brouwer L 2019 Magnetization current simulation of high temperature bulk superconductors using A–V–A formula based iterative algorithm method arXiv:1908.04640
- [28] Hellmann S, Calvi M, Schmidt T and Zhang K 2019 Optimization of short-period HTS staggered array undulators *Proc. MT26 (Vancouver)*
- [29] Durrel J H *et al* 2014 *Supercond. Sci. Technol.* **27** 082001
- [30] Moog E R, Dejus R J and Sasaki S Light Source Note: ANL/APS/LS-348
- [31] Clarke J A 2019 private communication